



University of HUDDERSFIELD

University of Huddersfield Repository

Hamomd, Osama, Alabied, Samir, Xu, Yuandong, Daraz, Alsadak, Gu, Fengshou and Ball, Andrew

Vibration Based Centrifugal Pump Fault Diagnosis Based on Modulation Signal Bispectrum Analysis

Original Citation

Hamomd, Osama, Alabied, Samir, Xu, Yuandong, Daraz, Alsadak, Gu, Fengshou and Ball, Andrew (2017) Vibration Based Centrifugal Pump Fault Diagnosis Based on Modulation Signal Bispectrum Analysis. Proceedings of the 23rd International Conference on Automation & Computing, (University of Huddersfield, 7-8 September 2017). ISSN 9780701702601

This version is available at <http://eprints.hud.ac.uk/id/eprint/33642/>

The University Repository is a digital collection of the research output of the University, available on Open Access. Copyright and Moral Rights for the items on this site are retained by the individual author and/or other copyright owners. Users may access full items free of charge; copies of full text items generally can be reproduced, displayed or performed and given to third parties in any format or medium for personal research or study, educational or not-for-profit purposes without prior permission or charge, provided:

- The authors, title and full bibliographic details is credited in any copy;
- A hyperlink and/or URL is included for the original metadata page; and
- The content is not changed in any way.

For more information, including our policy and submission procedure, please contact the Repository Team at: E.mailbox@hud.ac.uk.

<http://eprints.hud.ac.uk/>

Vibration based centrifugal pump fault diagnosis based on modulation signal bispectrum analysis

Osama Hamomd, Samir Alabied, Yuandong Xu, Alsadak Daraz, Fengshou Gu and Andrew Ball

Centre for Efficiency and Performance Engineering, University of Huddersfield, HD1 3DH, UK

Osama.Hamomd@hud.ac.uk F.Gu@hud.ac.uk

Abstract— This paper characterises vibration signals using modulation signal bispectrum method in order to develop an effective and reliable feature sets for detecting and diagnosing faults from both the bearings and impellers in a centrifugal pump. As vibration signals contain high level background noises due to inevitable flow cavitation and turbulences, effective noise reduction and reliable feature extraction are critical procedures in vibration signal analysis. Considering the modulation effect between rotating shaft and vane passing components, a modulation signal bispectrum (MSB) method is employed to extract these deterministic characteristics of modulating components in a low frequency band for diagnosing both the bearing defects and impeller blockages. Experimental results show that the diagnostic features developed by MSB allow impellers with inlet vane damages and bearing outer-race faults to be identified under different operating conditions. Not only does this new method produces reliable diagnostic results but also it needs a bandwidth about 1000Hz, rather than the high frequency bands around 10kHz used by conventional envelope analysis.

Keywords- Centrifugal pumps, fault diagnosis, power spectrum, MSB analysis

I. INTRODUCTION

A centrifugal pump is designed to achieve best performance at a specific combination of capacity, head, and speed, that is, the best efficiency point (BEP). Centrifugal pumps are used in many important industries such as petroleum refining process, petrochemical plant and power stations. Considering the criticality of these applications, the monitoring of the centrifugal pumps is necessary to ensure high-performance safety operations of pumps [1]. Therefore, many studies have been conducted in recent years with more advanced data analysis methods applied to the vibration of the pump. Nasiri et al [2] applied vibration analysis to detect cavitation in a centrifugal pump using a neural network system. The method provides an intelligent system to be used in condition monitoring of centrifugal pumps. Zhang et al. [3] intend a new method based on multi-scale entropy and adaptive neuro-fuzzy interference system conducted on electric motor bearings with three different fault categories of outer race, inner race and ball faults. Zhu et al. [4] proposed a new fault feature extraction method based on Intrinsic Mode Function, envelope sample entropy for rolling bearings fault diagnosis.

Berli Kamiel et al [5] proposed to develop a framework for impeller fault detection using multi sensor data collection and principal component analysis. Vibration signatures of normal and faulty impellers were collected from a Spectra Quest Machinery Fault Simulator. The

impeller fault was introduced by cutting two slots on the blade at two locations in the middle section of the blade, and four accelerometers were mounted on the pump on the volute case. Four statistical features (kurtosis, RMS, skewness, and variance) were extracted from time data which was previously separated into frequency bands or octaves.

Rafik Zouari et al [6] described a diagnosis system for centrifugal pumps that was developed in the framework of pump maintenance project using use neuro-fuzzy models. The system is based on vibration measurements, signal pre-processing and classification with pattern recognition approaches for detecting faults including misalignment, cavitation, partial flow, and air injection.

Saeid Farokhzad [7] presented an adaptive network fuzzy inference system (ANFIS) to diagnose the fault type of the pump. The pump conditions were considered to be healthy, broken impeller, worn impeller, leakage and cavitation. These features were extracted from vibration signals using the FFT technique. The features were fed into an adaptive neurofuzzy inference system as input vectors. Performance of the system was validated by applying the testing data set to the trained ANFIS model.

The works reviewed above are mainly based on statistical characteristics of vibration signals for detection and diagnosis. As these statistical characteristics are highly depends on the design features and applications of different pumps, these approaches generally are not so generalised for different applications. In addition the results often cannot be explained by engineering senses, making it difficult to convince the presence of faults at early stage. To overcome the shortcomings of the methods, this study focuses on developing detection and diagnostics using more deterministic features such as the vibration components associating with the pump rotor, bearing and impeller excitations. Furthermore, it emphasises on the diagnosis of early faults on the pump which are subject to different erosions including evitable cavitation turbulences and bearing fatigues.

II. VIBRATION FUNDAMENTALS OF CENTRIFUGAL PUMPS

A centrifugal pump has two main parts: the rotating element that consists of a shaft and an impeller and the stationary element that consists of the casing, casing box and bearing, and electrical motor with a cooling fan. Based on the pump working process, vibration can be understood as generated by both hydrodynamic and mechanical sources. Hydrodynamic sources usually cause fluid flow perturbation in the pump and facilitate interaction of the

rotor blades using nearby stationary objects, such as the volute tongue or guide vanes. Meanwhile, mechanical sources are caused by vibration of unbalanced rotating mass and friction in bearing and seals. These mechanisms of generating vibration cause the structure of the pump to vibrate. Moreover, General vibration responses to faults periodic with impeller and with bearing characteristic frequency Small differences and usually masked by random noises due to unsteady flows. From this perspective, the basic generating mechanisms for both structure-borne vibration and airborne noise are the same for a sealed pump system [8, 9].

III. EXPERIMENTAL FACILITY AND FAULT TESTS

The centrifugal pump under test can delivery up to 450 l/min of water under a pressure of 10bar when the driving motor operates at a rated speed of 2900rpm, the discharge flow can be adjusted by the discharge control valve to test the pump under different flow rate, allowing its vibration characteristics to be examined over its full operating ranges, Figure 1 shows the schematic diagram of test rig used in this experimental work.

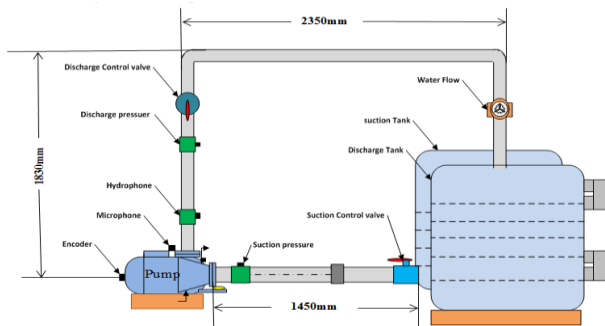


Figure 1 The schematic diagram of the experimental rig

A. Fault simulations

The experiment was carried out based on two different cases healthy one where's the second are bearing outer-race defect + small and large impeller blockage faults. One bearing and impeller are healthy and taken as the baseline form comparison. Figure 1-2 presented out the photo of defect on the inlet impeller blockage and figure 1-3 shows the bearing outer race defect. Were tested under full constant speed (2900) rpm and nine different flow rats (0, 50,100,150,200, up to 450) each test acquired data at fourthly seconds record.



Figure 1 2 The impeller inlet blockages

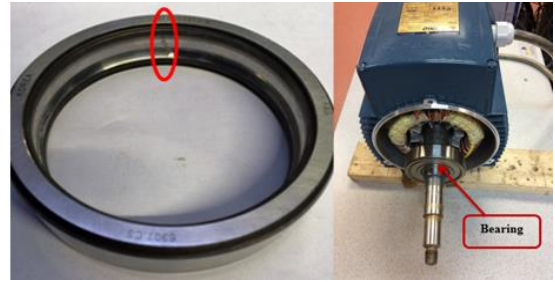


Figure 1 3 Defects subjected on the bearing outer-race and it's position

IV. SPECTRUM ANALYSIS BASED DIAGNOSTICS

To show the basic characteristics of pump vibration, this studies the spectrum for the bearings and impellers fault under different conditions and flow rats.

A. Spectrum comparison

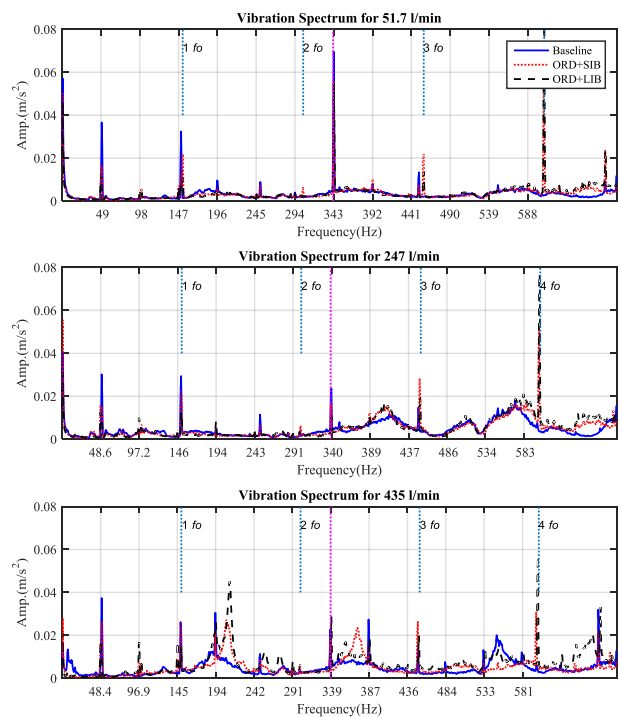


Figure 1-4 Vibration spectrum in the low frequency range

Figure 1-4 shows the vibration spectrum in a low frequency under three typical flow rates: Above 400 l/m flow rate, around 250 l/m flow rate and low flow 50 l/m for the baseline and the defects on Bearings and impeller. It can be observed that the vibration spectrum exhibits clear broadband due to flow turbulence and visible discrete components due to the interactions between vane and flow. In addition, the discrete components appear at the frequencies of 147 Hz and second harmonics 292 Hz but also at the shaft frequency 48.4.1Hz and its harmonics. Moreover, the 4f_o it's the 4 harmonics of bearing outer-race which have both fault appear at the same harmonics. The shaft related commoners all most for three different flow rats, especially at its harmonics may indicate the asymmetry between vanes and hence could be useful for reveal the faults. It is difficult to find the characteristic frequencies for making diagnostics. However, these mechanisms of generating vibration cause the structure of the pump to vibrate. Moreover, general vibration responses to faults periodic with impeller and with bearing

characteristic frequency Small differences and usually masked by random noises due to unsteady flows.

B. Detection and Diagnosis of Bearing Faults

Figure 1-5 shows the spectrum of vibration data collected on pump bearing for three different cases stated as (BL, ORD+SIB, ORD+LIB), under different flow rates from 50 l/m up to 400 l/m. It can be observed that the results of the three cases at graphs from $1f_o$ to $4f_o$ which can be observed that from the two bottom graphs $3f_o$ and $4f_o$ shows that the both bearing faults can be separated from the healthy case with more distinctively less noise contamination for all three cases as shown in Figure 1-5. which is spirited over the bearings with large impeller blockage fault at all flow rats range. It shows that the amplitudes show the change with high flow rates above 300 for (SIB) but allows the (LIB) faulty to be differentiated fully, because of the influences of the wideband noise. Moreover, it is consistent with the changes of the performance characteristics. As the flow pressure is lower, the vibration goes higher for the bearing with a large impeller blockage faults and vice versa for the bearing with a small blockage fault.

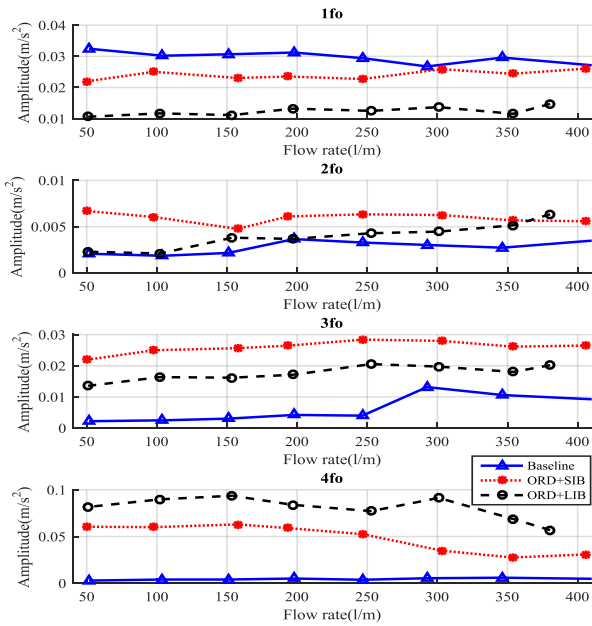


Figure 1-5 Compared of diagnostic results for bearing faults using spectrum

C. Detection and Diagnosis of Impeller Faults

The diagnostic features extracted as shown in Figure 1-6 for three different cases stated as (BL, ORD+SIB, ORD+LIB) under different flow rats from 50 l/m to 400 l/m. It can be observing that the results of the three cases at graphs from $1f_r$ to $7f_r$ which cannot be separated. In additional when marriage the middle row $5f_r + 3f_r$ it can shows that the both impeller faults can be separated from the healthy case with more distinctively less noise contamination for all three cases. Especially, their nonlinear coupling can be further identified, which is spirited over the large impeller blockage fault at the first 4 harmonics of shaft rotating frequency and the first vane passing frequency. It shows that the amplitudes show less change with low flow rates under 300 for (SIB) but allows

the (LIB) faulty to be differentiated fully, because of the influences of the wideband noise. Moreover, it is consistent with the changes of the performance characteristics. As the flow pressure is lower, the vibration goes higher for the large impeller blockage fault and vice versa for the small blockage fault.

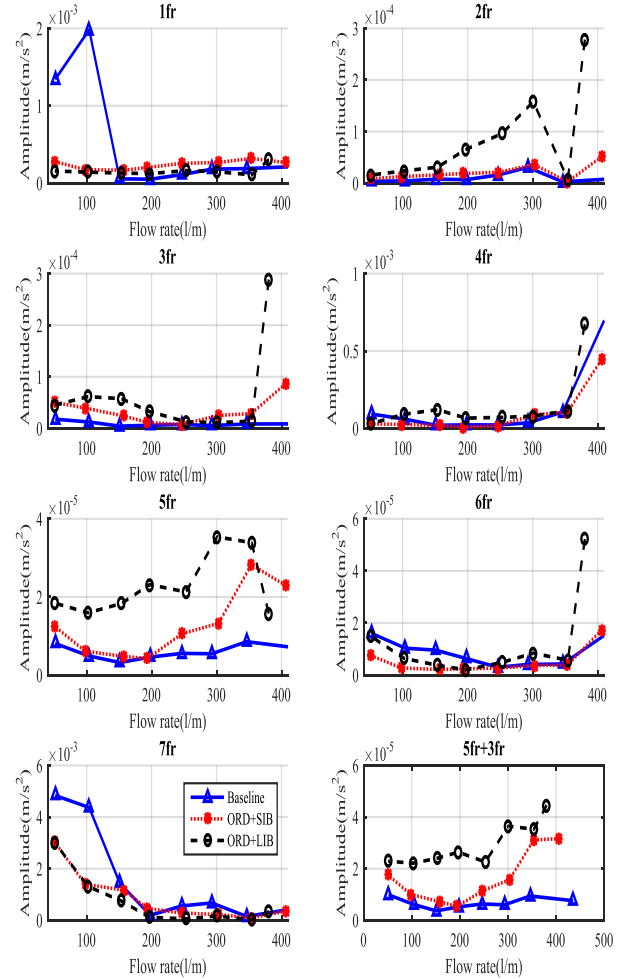


Figure 1-6 Compared of diagnostic results for impeller faults

V. MSB ANALYSIS BASED DIAGNOSTICS

This section aims to study the Modulation signal bispectrum analysis based diagnostics of the bearings and impellers fault under different conditions and flow rats.

A. Bearing Detection and Diagnosis

1) Characteristics of MSB

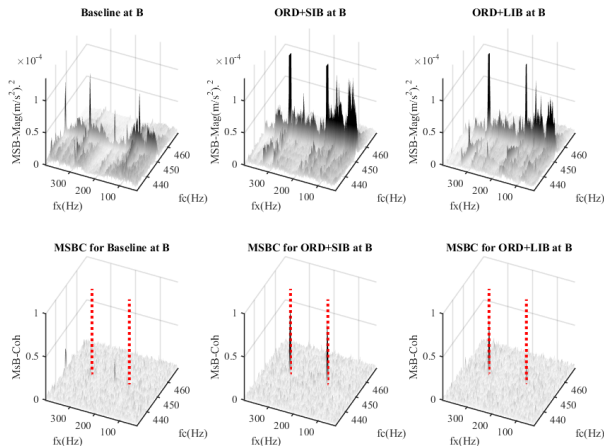


Figure 1-1 MSB magnitude and MSB coherence of vibration signals for bearing different cases at flow rate 250 l/min

Figure 1 7 shows the MSB magnitude and MSB coherence of vibration data collected on pump bearing for three different cases stated as (BL, ORD+SIB, ORD+LIB). The MSB magnitude results of the three graphs of top row show less noise contamination for all three cases. Especially, their nonlinear coupling can be further identified by the corresponding MSB coherence in the three graphs of bottom. Subsequently, the average of the two components obtains the results from MSB coherence detector as shown on the three graphs of bottom row, which are coloured, red. In additional, the results show clear peaks at outer race fault frequency and its second harmonic, when comparing with the baseline case, which has no fault induced to. In the meantime, both results show distinctive differences between three cases in that the outer race faults causes higher peaks because of higher mechanical pulses during to the defect whereas the baseline induces very smaller pulses and hence lower MSB coherence peaks.

2) Diagnosis of Bearings Based on MSB Entropies

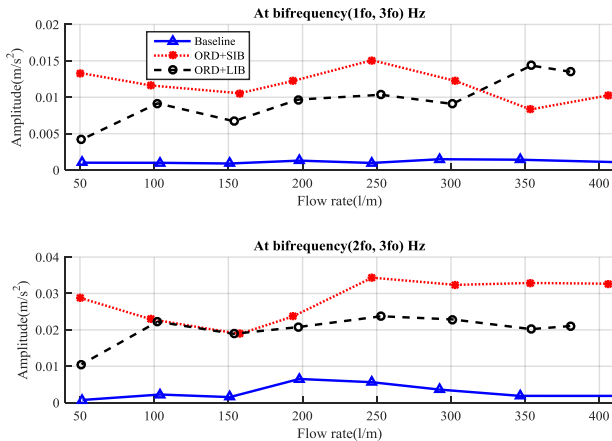


Figure 1 8 Compared of diagnostic results for bearing faults

The diagnostic features extracted as shown in **Error! Reference source not found.** For three different cases stated as (BL, ORD+SIB, ORD+LIB). under different flow rates from 50 l/m up to 450 l/m. It can be observing that the results of the three cases at graph of the top row from $1f_0$ and $3f_0$ which can be observed that the both bearing faults can be separated from the healthy case with more distinctively less noise and amplitudes show less change with high flow

rates above 300 l/m. contamination for all three cases as shown in **Error! Reference source not found.** In additional it can be observed that from the bottom graph $2f_0$ and $3f_0$ shows that better result at the high flow rates and Amplitude, which is spirited over the bearings fault at the high flow rates of shaft rotating frequency. It shows that the amplitudes change with high flow rates above 250 but allows the (ORD) faulty to be differentiated fully at the second and third harmonics, because of the influences of the wideband noise. Moreover, it is consistent with the changes of the performance characteristics. As the flow pressure is lower, the vibration goes higher for the (ORD+LIB) fault and vice versa for the (ORD+SIB).

B. Impeller Detection and Diagnosis

1) Characteristics of MSB

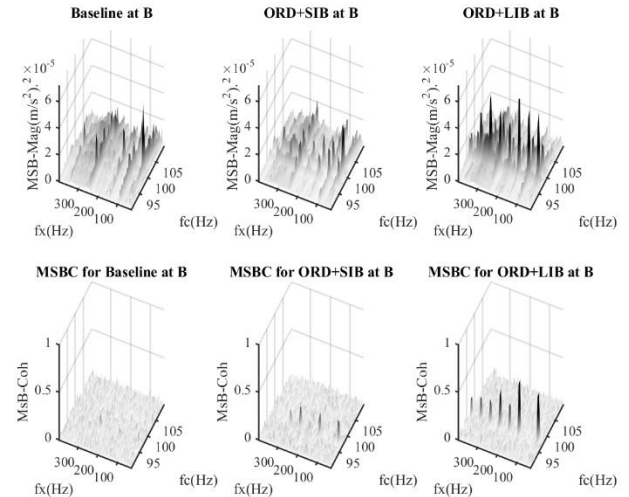


Figure 1-2 MSB magnitude and MSB coherence of vibration signals for impeller different cases at flow rate 250 l/min

To improve the diagnosis performance, the MSB is applied to suppress the wideband noise and hence to enhance the discrete components. Figure 1-2 representative of MSB in the low frequency range. The MSB magnitude results of the three graphs of top row show less noise contamination for all three cases. Especially, their nonlinear coupling can further have identified by the corresponding MSB coherences in the three graphs of bottom. Subsequently, the average of the two components obtains the results from MSB coherence detector as shown on the three graphs of bottom row in Figure 1-2. The results show clear peaks at small impellers blockage fault frequency and its second harmonic, when comparing with the baseline case, which has no fault induced to. In addition, both results show distinctive differences between three cases in that the large impeller fault causes higher peaks because of higher mechanical and hydraulic asymmetric pulses whereas the small impeller fault induces smaller pulses and hence lower MSB coherence peaks.

2) Diagnosis of Impellers Based on MSB Entropies

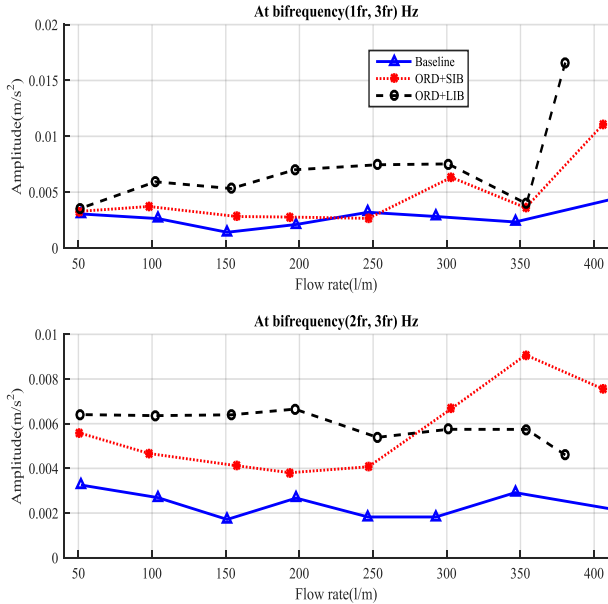


Figure 1-3 Compared of diagnostic results for impeller faults

The diagnostic features extracted as shown in Figure 1-3. For three different cases stated as (BL, ORD+SIB, ORD+LIB). under different flow rates from 50 l/m up to 450 l/m. It can be observing that the results of the three cases at graph of the top row from $1f_r$ and $3f_r$, which can be observed that the both impellers fault can be separated from the healthy case with more distinctively less noise and high amplitudes show less change with high flow rates above 300 l/m. contamination for all three cases as shown in Figure 1-3. In additional it can be observed that from the bottom graph $2f_r$ and $3f_r$ shows that better result at the high flow rates and Amplitude, which is spirited over the impellers blockage at the high flow rates of shaft rotating frequency. It shows that the amplitudes change with high flow rates above 250 but allows the (LIB) faulty to be differentiated fully at the second and third harmonics, because of the influences of the wideband noise. Moreover, it is consistent with the changes of the performance characteristics. As the flow pressure is lower, the vibration goes higher for the large impeller blockage fault and vice versa for the small blockage fault.

VI. CONCLUSION

It starts with an in-depth examination of the vibration excitation mechanisms associated with each type of common pump faults including impeller leakages, impeller blockages, bearing inner race defects and bearing outtrace defects. Subsequently, fault diagnosis was carried out using popular spectrum analysis, and more advanced MSB analysis. These methods all can successfully provide

correct detection and diagnosis of the faults which are induced manually to the test pump.

On the other hand, it has found that the MSB analysis allows both impeller and bearing faults to be detected and diagnosed. Especially, when the pump operated with compound faults both the fault types and severity can be attained by the analysis with acceptable accuracy for different flow rates. This high performance of diagnosis is due to that MSB has the unique capability of noise reduction and nonlinearity demodulation. Moreover, MSB diagnosis can be a frequency range lower than 2 times of the blade pass frequency ($<1\text{kHz}$), meaning that it can be more cost-effective as it demands lower performance measurement systems. which is obtained by averaging MSB peaks in low frequency range, can make good differentiation of the impeller defects and the bearing defect from the healthy ones because its capability of wideband noise suppression, demonstrating that the proposed method is effective. Moreover, the discrete components caused by the interaction of flow, impeller and bearing show more definitive change due to the defects. In particular, the amplitudes at vane passing frequency and the higher order harmonics at shaft frequency can be effective features for the detection and diagnosis of the fault severity.

REFERENCES

- [1] Juneja, B.L., G.S. Sekhon, and N. Seth, Fundamentals of metal cutting and machine tools. 2003, New Delhi: New Age International Ltd. Publishers.
- [2] Nasiri, M.R., M.J. Mahjoob, and H. Vahid-Alizadeh. Vibration signature analysis for detecting cavitation in centrifugal pumps using neural networks. in Mechatronics (ICM), 2011 IEEE International Conference on. 2011. IEEE.
- [3] Zhang, L., et al., Bearing fault diagnosis using multi-scale entropy and adaptive neuro-fuzzy inference. Expert Systems with Applications, 2010. 37(8): p. 6077-6085.
- [4] Zheng, J., J. Cheng, and Y. Yang, A rolling bearing fault diagnosis approach based on LCD and fuzzy entropy. Mechanism and Machine Theory, 2013. 70: p. 441-453.
- [5] Kamiel, B., et al., Impeller Fault Detection for a Centrifugal Pump Using Principal Component Analysis of Time Domain Vibration Features. Department of Mechanical Engineering, Universitas Muhammadiyah Yogyakarta, Indonesia, 2005.
- [6] Zouari, R., S. Sieg-Zieba, and M. Sidahmed, Fault detection system for centrifugal pumps using neural networks and neuro-fuzzy techniques. Surveillance, 2004. 5: p. 11-13.
- [7] Farokhzad, S., et al., Artificial neural network based classification of faults in centrifugal water pump. Vibroengineering, 2012. 14(4): p. 1734-1744.
- [8] Florjancic, S. and A. Frei. Dynamic Loading on Pumps—Causes for Vibrations. in 10th International Pump Symposium. 1993.
- [9] Black, H., Effects of hydraulic forces in annular pressure seals on the vibrations of centrifugal pump rotors. Journal of Mechanical Engineering Science, 1969. 11(2): p. 206-213.